Journal of Electrical Engineering, Electronics, Control and Computer Science – JEEECCS, Volume 12, Issue 41, pages 31-36, 2026

Analytical Design of a Microcontroller-Based Hearing Aid Device

Adedotun Oluwakanyinsola Owojori
Dept. of Electrical and Electronics Engineering
Federal University of Technology, Akure
Akure, Ondo State, Nigeria
aoowojori@futa.edu.ng

Abstract **– According to epidemiological study hearing disability is critical if it diminishes to at least 40 dB at frequency ranges of 0.5 kHz to 4 kHz. This form of impairment impact one's perception of its immediate surroundings leaving the person to develop or cultivate other means of interaction to the surrounding. To some extent, the level of impairment could be catered for by a hearing aid device for partly impaired persons. However, proper analysis of such system is required to allow or accommodate audio reception. The sectional design consideration aligns with human hearing specifications and with the Estimated Mean Average (EMA) digital filtering algorithm a suitable system is developed. The design adopts the use of a microcontroller-based system interconnected with other hardware components for trapping signals and preprocessing the signals.**

Keywords-hearing aid; impairment; sound waves; hearing disability; filtering algorithm

I. INTRODUCTION

The ears as shown in Figure 1 is one of the organs that affects the perception of life which makes it unparallelly important to human existence. It is one of the mediums through which human relates with its environment via sound waves. The art of hearing requires correct interpretation of sound waves in the human brain to give appropriate responses within acceptable audio ranges. However, malfunction of such organ termed hearing loss can affect the way individuals perceive its environment which over the years has contributed to the level of stigmatization amongst people with ear impairment. It has been estimated as the commonest sensory disability and the third greatest contributor to the global burden of disease [1] which has been observed to affect low to middle income countries. Hence, the hearing aid device serves as means of rehabilitation [2] which needs to be supplied at a low cost and meet 10% of global availability [1].

According to [3], [4] hearing impairment are either total (anacrusis) or partial with patients having a hard to hear scenario such a patient can pick up fractional sounds. The level of impairment could be catered for by means of a hearing aid device which preprocesses the signal received, amplifies it then transfers to the ears. However, taking advantage of the digital signal processing and reduced filter coefficient design of which varying range of hearing defects can be addressed becomes plausible for adaptive design [4], [5]. The result of which involves obtaining an optimal response function which mimics the acoustic response of the meatus implemented on a real time controller device at optimized power [4].

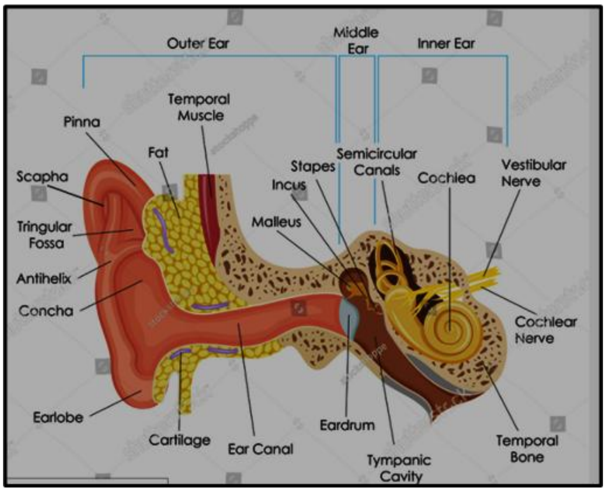

Figure 1. Anatomy and Physiology of the human ear [6]

Earlier design of electronic hearing aid was bulky used in movies or talking pictures entertainment sectors. Later, in the 1950s telecoil was used to achieve an assistive listening system. These include the introduction of the cochlea implant which became a big milestone achieved as the log-domain analog based implant device and had birthed other devices which utilizes digital domains with optimized form factor. The challenge of analog design is its ability to amplify residue signal in an all-pass band. In a bit to solving this challenge, a hearing aid response function is modeled and processed digitally so as to facilitate an optimum adaptation of the auditory signal while passing it through an appropriate filter.

With the different functions of the outer, middle and inner section of the human ear [4], [6] as shown in Figure 2, it is observed that the base of the cochlea in the inner ears responds to high frequency sounds, while the apex responds to low frequency sounds. Most common hearing impairment in childhood is transient conductive in nature due to tympanic effusion in the eardrum while congenital, permanent and bilateral hearing loss is prevalent with children. Adults however, experience a sensorineural hearing loss due to old age (presbycusis). Permanent conductive or combined hearing loss does exist due to the chronic otitis media and the acoustic trauma [7], [8].

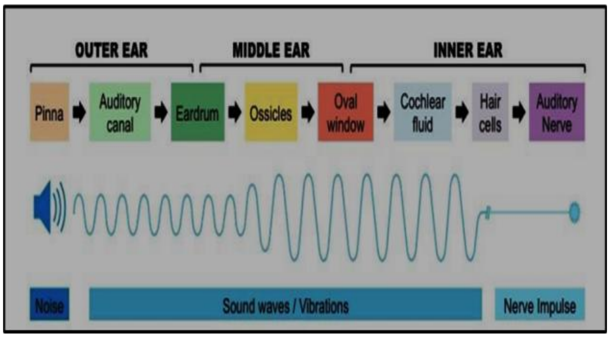

Figure 2. Illustration of Sound Travel in the Ear [6]

For effective hearing to occur acoustic energy or sound wave is transmitted through the canal to hit the eardrum from which the ossicle bones convert the acoustic vibration energy into mechanical energy. The middle ear bones mechanically amplify sound and compensate mismatched impedance. The cochlear creates a fluid in form of a hydrodynamic energy causing the ‘organ of Corti’ to shear against the hair cells generating an electrochemical signal sent through the auditory nerves to the brain [6], [9]. However, a shift in the bone conduction threshold by up to 50 dB a loss of nonlinear reinforcement with impaired frequency sensitivity occurs [10], [11].

TABLE I [1] World Health Organisation (WHO) classification of the severity of hearing impairment, summarizes a range of impairment level and electroacoustic performance requirement parameters for manufacturing hearing aid devices. The guidelines are reflected on current technical standard performance as corroborated by Figure 3 showing the Equi loudness contour of sound pressure in dB [12], [13].

TABLE I. WORLD HEALTH ORGANISATION (WHO) CLASSIFICATION OF THE SEVERITY OF HEARING IMPAIRMENT [1]

Hearing aid Parameters	Minimum Requirement
Maximum OSPL (90)	100-130 dB SPL $\pm$ 4dB
OSPL (90) at 1 kHz	90-124 dB SPL $\pm$ 4dB
Maximum Full-on acoustic gain	45-67 dB SPL $\pm$ 5dB
Full-on acoustic gain at 1 kHz	42-70 dB SPL $\pm$ 5dB
Basic frequency response	200-4500 Hz 200-2000 Hz @ $\pm$ 4dB SPL 2000-4500 Hz @ $\pm$ 6dB SPL
Total harmonic distortion at 70 dB SPL input	500 Hz < 8%; 800 Hz < 8%; 1500 Hz <2%
Equivalent input noise @ 1 kHz	<30 dB SPL @ 1 kHz
Battery current drain	$\leq$ 1 Ma
Battery life	2-3 weeks
Telecoil sensitivity	$\geq$ 75 dB at 10 mA/m

The ANSI S3.22-2009/IEC 60118—7 measures are used to estimate the amount of amplification appropriate for the degree of hearing loss. This measure must take care of adult, children [14], must be able to withstand mild shock impact, be software compactable and easily interfaced with affordable hearing aid device. The OSPL represents the output sound pressure level which represents the maximum output sound pressure level the hearing aid device can be exposed to so it does not amplify sound beyond hearing thresholds and it’s a function of frequency in kHz.

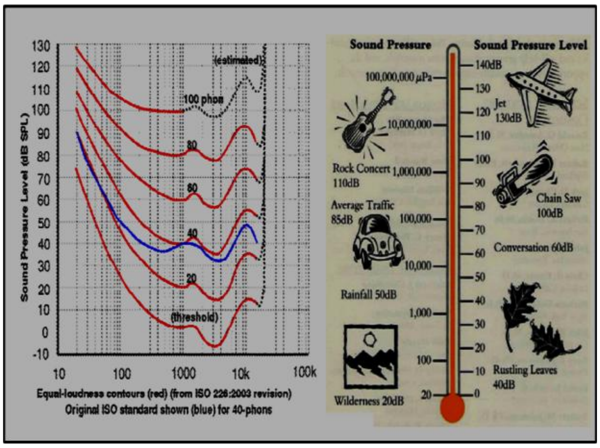

Figure 3. Decibel scale [12], [13]

System and software compatibilities are key components designer look out for which distinguishes the analog design from the digital design technologies [15], [16], [17]. Although recent trends reflect reduced form factor (scalable) design, wireless enabled, low cost and reconfigurable system design [4], [18]. Introduction of the digital signal processing (DSP) concept into hearing aid design allows advanced processing algorithms to be implemented, sensor interfacing and feedback management extension [4], [5], [19].

II. EXPERIMENTAL SETUP

In order to carry out the analytical design of this system the individual component of the hearing aid device is considered from the directional microphone to the output stage via a headset suitable of stimulating the auditory nerves to pick up the signal and translate to the brain.

A. Sensing Unit

With weak signals extracted from useful audio signal as against the surrounding environment, a miniaturized electret microphone integrated with an onboard preamp circuit is used to receive a signal of approximately 250 mV peak value and amplifies it to 2.5 V peak value. The audio module has an external power source of 5 V which powers the amplifier IC (LM 393). The modeling of the system was done using the non-inverting amplifier configuration to mimic the audio signal module expressed in (1).

$$\frac{v_0}{v_{in}} = 1 + \frac{R_f}{R_{in}} \tag{1}$$

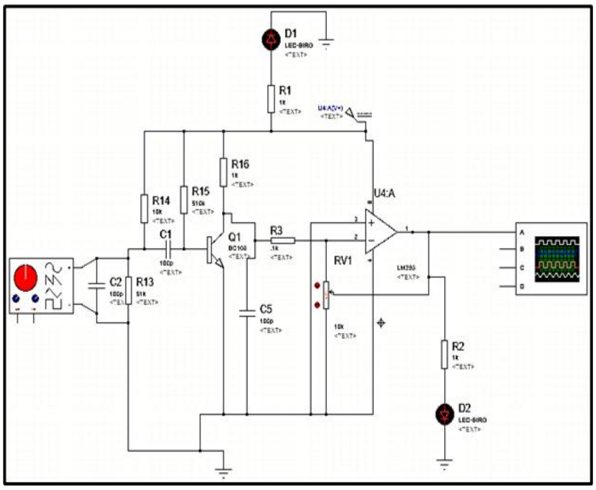

Figure 4. Illustrates the overall sensing unit of a hearing aid device

a) Signal Input Stage

Analysis of this system shown in Fig. 4 shows a filter-based input configuration with an interaction between an alternating current (AC) signal and a direct current (DC) bias. This is done to ensure the signal is placed within a set operating range. Applying superposition theorem and the DC source is grounded, R_{13} and R_{14} are placed parallel to C_2. Conventionally, at high frequency the capacitor should act as a short circuit grounding all the signals but, in this case, it only acts as a filter while it passes the signal as expressed in (2) with time constant $\tau \approx 0.836\mu s$ [20], [21]. On the other hand, the DC is active while the analog signal from the signal generator is disconnected. This sets an operation range or bias for the input signal of which the capacitor C_2 is open circuited to DC supply and the output is expressed in (3).

$$v_{ac} = v_0 e^{-\frac{t}{CR}} \tag{2}$$

$$V_{dc} = \frac{R_{13}}{R_{13} + R_{14}} \times V_{cc} \tag{3}$$

$$v(t) = v_{ac} + V_{dc} \tag{4}$$

where C is C_2 and R is the parallel equivalent of R_{13} and R_{14}.

The equivalent signal expressed in (4) which is the algebric sum of the outputs is then passed through a coupling capacitor C_1 which allows AC signal to pass to the next stage while blocking DC voltages at thesame time allows connection to an amplifier source and load without altering the DC operating points.

b) Amplification Stage

Contained internally in the audio module is a cascade amplifier of a Common Emitter (CE) based Bipolar Junction Transistor (BJT) and an inverting operational amplifier. With DC analysis of the transistor (5)-(6) were obtained.

$$I_B = \frac{V_{cc} - V_{BE}}{R_{15}} \tag{5}$$

$$I_c = \beta I_B \tag{6}$$

Since $V_{BE} \approx 0.6V$ (base-emitter voltage) and $I_B > 0$ (base current), the BJT transistor operates at the quiescent point or operating mode however, the output gain of the transistor is expressed in (7)-(8) using the small signal equivalent or AC analysis. In this case the DC source is grounded hence the output voltage is observed at the collector terminal of the Q1 (BJT) component.

$$A_{v1} = -g_m R_L \tag{7}$$

$$g_m = \frac{I_c}{25m} = 40 I_c \tag{8}$$

where R_L is R_{16} representing the load resistance for the first amplifier stage, I_c is the collector current.

With capacitor C_5 at the output connected to ground serving as a lowpass filter component in the given configuration, a resistor R_3 is used to couple the output of the first amplifier stage to an inverting operational amplifier (second stage). The amplifier gain of the second stage is expressed in (9).

$$A_{v2} = -\frac{R_f}{R_{in}} \tag{9}$$

$$A_v = A_{v1} \times A_{v2} \approx 10 \tag{10}$$

Where R_f represented as RV1 is a variable resistor or potentiometer and R_{in} is R_3. The overall amplifier A_v in (10) gives an effect of a non-inverting amplifier as expressed in (1) and has an overall amplification gain of 10, with output voltage 2.5 V all contained in an off-the-shelf module. Light Emitting Diodes (LED) are introduced to the input and output terminal of the circuit as indicators for flow of current.

B. DC Offset Unit

The DC-offset configuration illustrated in Figure 5 is introduced by a coupling capacitor C_7, then a resistor configuration (R_{17} and R_{18}) immediately after the amplification stage, this is targeted to position the lowest value of the signal to 0 V. Such configuration is effective for signals inputted to the microcontroller. The circuit configuration involves the modification of a voltage divider circuit with the output value or offset scaled up to negate the negative signal in the system which is suitable for the microcontroller as expressed in (11)-(13). Shown in Figure 6 is a parallel capacitor C_1 introduced across R_{18} which serves as a filter creating a time constant discharge for the amplifier output signal and the microcontroller unit.

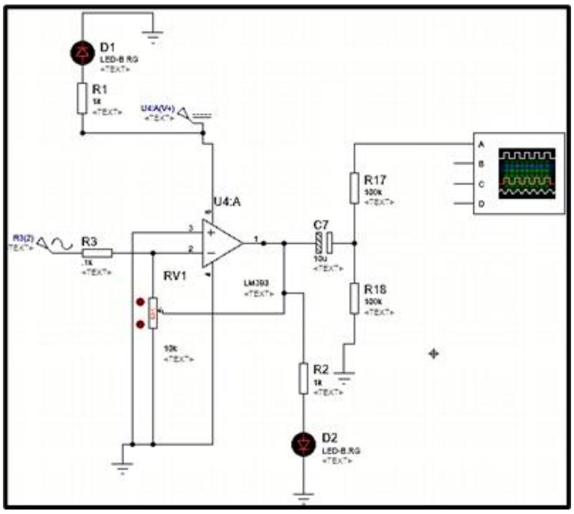

Figure 5. Introduction of DC-offset configuration

$$v_0(t) = A_v \times v(t) \tag{11}$$

$$v_0(t) = \frac{R_{18}}{R_{17} + R_{18}} v_{01} \tag{12}$$

$$v_{01} = (1 + \frac{R_{17}}{R_{18}}) \times v_0(t) \tag{13}$$

C. Controller Unit

The output from the DC-offset configuration (v_{01}) is then received through a 100 pF coupling capacitor to the A0 (Analog) pin of a microcontroller. Based on the instruction code set in the microcontroller the analog input is first digitize via an inbuilt analog to digital converter (ADC) as expressed in (14)-(15). With a bias voltage between 5-12 V and a reference voltage of 5 V the ADC can be set and with a chosen bit (B), the signal resolution can be obtained [17], [22], [23].

$$N = 2^B \tag{14}$$

$$C_{val} = \frac{(v_{in} \times v_{ref})}{2^B - 1} \tag{15}$$

With the Arduino analog filter library and the complementary filter algorithm deployed in (16), the microcontroller is able to eliminate all background noise above 20 kHz and below 20 Hz. After the conversion, the Arduino Nano microcontroller manipulate the serial communication signal to a digital based parallel output expressed through I/O terminals D_9-D_{12}.

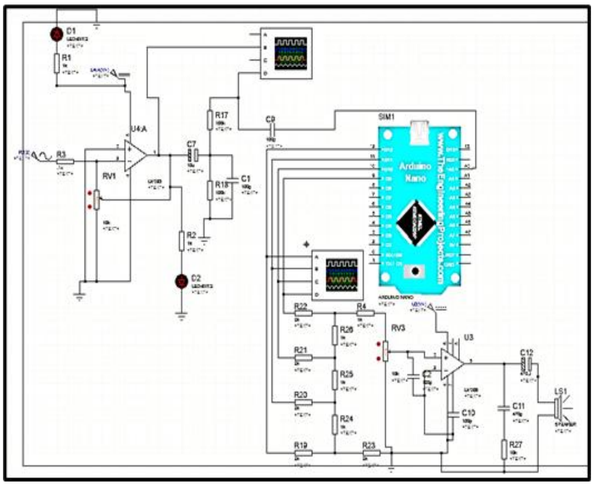

Figure 6. System Interface with Controller and Output Signal Acquisition Unit

$$EMA_{new} = EMA_{old} \times (1 - (\frac{smoothing}{1+d}))...$$

$$... + Value_{new} \times (\frac{smoothing}{1+d}) \tag{16}$$

where $(\frac{smoothing}{1+d})$ is the smoothing coefficient, EMA_{old} representing high frequency component and $Value_{new}$ representing low frequency component [4].

The complementary filter besides been an exponential moving average estimator finds application in fintech historical data analyisis and robotic pitch angle estimation. Its algorithm is designed to add two filtered signals together capturing the real-time drift or short comings of one and using the robustness of the other filtered signal to stablilize the whole system. This can be viewed in the interraction between the lowpass filter as observed in accelerometer sensors and highpass filter in gyroscope sensors as shown in Figure 7 of a motion tracking system as could be applicable in the hearing aid system deployed to manipulate the frequency level.

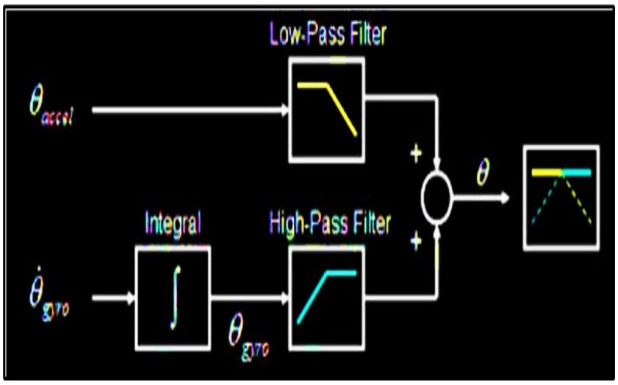

Figure 7. Complementary filter model of a gyro sensor [24]

D. Digital to Analog Converter (DAC)

The digital parallel communication obtained from the microcontroller I/O output terminal responds to the filter algorithm and with the $(R-2R)$ ladder circuit, the equivalent digital signal can be converted to analog signal. Adopting superposition theorem, the overall output equivalent realised across potentiometer (RV3) is expressed in (17)-(18) where the output D_9-D_{12} are as identified in the Figure 6 of the system design

$$v_0 = \sum_{i=1}^{n} v_{0i} \tag{17}$$

$$v_0 = \frac{D_{12}}{2^4} + \frac{D_{11}}{2^3} + \frac{D_{10}}{2^2} + \frac{D_9}{2^1} \tag{18}$$

From the expression it is observed that a base 2 equivalent of the digital signal is used to obtain the analog signal with signal D_9 been the least significant bit (LSB).

E. Output Amplification Unit

The output amplification stage simply represents a comparator circuit with the input fed from the $(R-2R)$ ladder circuit through the potentiometer (RV3) which represents the gain control. The result from the amplification gives an inherent open loop differential amplification. The circuit requires an operational amplifier LM386 biased by a 9V power supply and in operation in the positive saturation region the output is approximately estimated as (19).

$$v_0 = v_{cc} - 0.2 \tag{19}$$

The output however is further filtered via a resistor capacitor (RC) circuit configuration before connecting it to a speaker.

III. Results and Discussion

In simulation mode, different subsections where identified this serves as a model base for the hardware implementation where real-time audio signal was input to the system. This shows an extension of [4] by further elaborating the design analysis where a signal generator used as input signal was set to a peak-to-peak voltage of 250 mV at a frequency of 3.4 kHz within the audio range as shown in Figure 8.

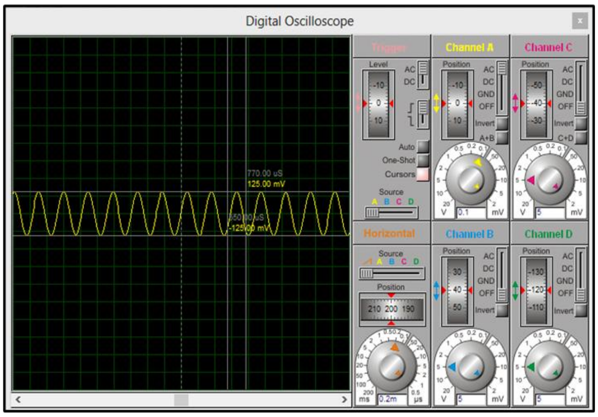

Figure 8. The signal generator input to the audio sensing unit

The output of the overall sensing unit was observed to have an attenuated signal of 46 mV peak value as shown in Figure 9 while the input signal remains the same. This expresses a simulation approximation with respect to physical component connections. The block level analysis shows similar concept with [25] which gave a software analysis in Multisim and evaluated the frequency response gain measurement of the amplifier.

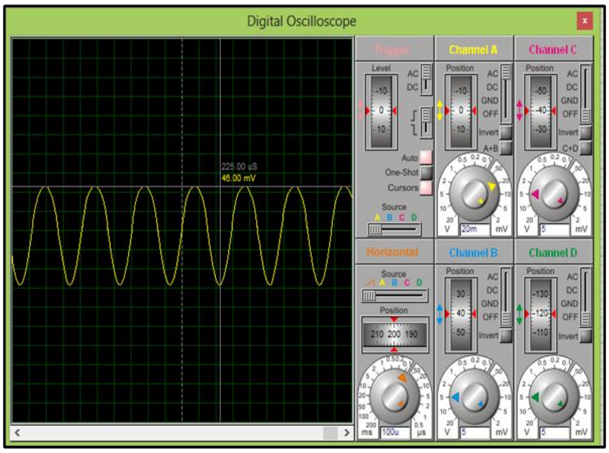

Figure 9. Overall sensing unit

With the system simply modified to accommodate the DC offset an output response was observed this was done to eliminate the negative swing and prepare the signal as input to the Arduino microcontroller. The digitized signal output was also observed from the microcontroller I/O terminal D_9-D_{12} which simply illustrates a conversion from serial communication to parallel communication.

Figure 10 illustrates the frequency response of Figure 4 as the response can only be obtained in parts due to some critical component such as light emitting diode (LED), Arduino microcontroller unit, and speaker which needed to be isolated. A probe is introduced at the output terminal and comparing its signal with the input reference signal a magnitude plot having a peak of -20dB and operating frequency >100 kHz to few 1 MHz at 0dB/dec. At low frequency from 10 mHz to <1 Hz the magnitude plot has a rate of +40dB/dec and from 1 Hz to 100kHz it has a rate of +20dB/dec whereas at high frequency 10 MHz to 10 GHz the rate is -60dB/dec.

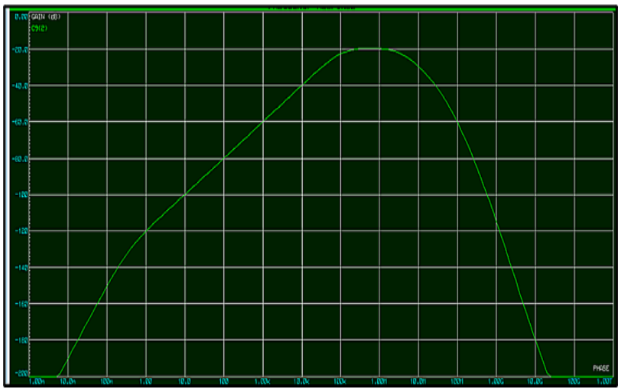

Figure 10. Frequency response of the sensing circuit

ACKNOWLEDGMENT

The author appreciates Labcenter Electronics for the accessible use of Proteus Design Suite 8.4 software and Arduino IDE for validating the C-code generated via simulation for easy deployment of .HEX code into the real-life microcontroller.

CONCLUSION

This paper had illustrated how to analyze, design and construct a microcontroller-based low-cost hearing aid devices in anticipation of the implementation stage design. Digital signal processing stage was introduced through an ATmeag328P microcontroller on an Arduino which is programmed in C as instruction code to filter out irrelevant frequencies based on the complementary filter algorithm, outputting a digitized signal through the I/O terminal of the controller and finally the frequency response analysis of the intermediate system which serves as a foundation for signal analysis with application in control/digital signal analysis. Future researches seek to elaborate on the frequency analysis using specialized software to achieve key performance indicators.

REFERENCES

[1] WHO, "Preferred Profile for Hearing-aid Technology suitable for low- and middle-income countries," 2017. ISBN 978-92-4-151296-1.

[2] R. J. H. Smith, "The Hearing-Impaired Patient: What the Future Holds. Human Genetics." 141(3-4), pp.307-310, 2022. https://doi.org/10.1007/s00439-022-02447-8.

[3] I. Holube, and V. Hamacher, "Hearing-aid technology." Communication Acoustics, pp.255-276, 2005. https://doi.org/10.1007/3-540-27437-5_10.

[4] I. A. Olajide, A. O. Owojori, and A. S. Durojaye, Design of a Programmable Hearing Aid Device. Advance Journal of Science, Engineering and Technology (Adv.J..Sci.Eng.Tech), 10(9), pp.1-15, 2025. https://doi.org/ 10.5281/zenodo.17055201.

[5] K. Priya, and P. Eswaran, Design and Implementation of Programmable Hearing Aid using FPAA. 2, pp.6-17, 2014.

[6] V. Kumar, Ear-Structure and Function. 2014. https://www.scribd.com/document/403938324/Ear.

[7] T. Zahnert, The Differential Diagnosis of Hearing Loss. Deutsches Arzteblatt International (Dtsch Arztebl Int), 108(25), pp. 433-444, 2011 https://doi.org/10.3238/arztebl.2011.0433.

[8] B. Ohlenforst, A. A. Zekveld, E. P. Jansma, Y. Wang, G. Naylor, A. Lorens, and S. E. Kramer, "Effect of Hearing Impairment and Hearing aid Amplification on Listening Effort. A Systematic Review." Pp. 267-281. 2017.

[9] J. R. Desjardins, and K. A. Doherty, "The Effect of Hearing Aid Noise Reduction on Listening Effort in Hearing-Impaired Adults." (Edwards 2007), pp. 600-610, 2014. https://doi.org/10.1097/aud.0000000000000028.

[10] P. A. Korczak, D. Kurtzberg, and D. R. Stapells, "Effects of Sensorineural Hearing Loss and Personal Hearing Aids on Cortical Event-Related Potential and Behavioral Measures of Speech-Sound Processing." 26(2), pp. 165-185, 2005. https://doi.org/10.1097/00003446-200504000-00005.

[11] B. W. Y. Hornsby, "The Effects of Hearing Aid use on Listening Effort and Mental Fatigue Associated with Sustained Speech Processing Demands." 34(5), pp.523-534, 2013. https://doi.org/10.1097/aud.0b013e31828003d8.

[12] R. V. Hartley, "Bell Laboratories – The Decibel Unit." 1928. https://web.facebook.com/groups/heyaudiostudent/posts/4315950448459745/?_rdc=1&_rdr.

[13] J. Charbonneau, C. Novak, and H. Ule, "Loudness Prediction Model Comparison using the Equal Loudness Contours. Canadian Acoustics." 37(3), pp. 64-65, 2009.

[14] L. E. Humes, and V. Krull, "Hearing aids for adults. Evidence-based practice in Audiology." Chapter 4, 2012

[15] A. E. May, L. J. Upfold, and J. A.Battaglia, "The Advantages and Disadvantages of ITC, ITE and BTE hearing aids: Diary and interview reports from elderly users." 5364 (February), 2016. https://doi.org/10.3109/03005369009076570.

[16] S. Venkateswar, and N. Mehendale, "Smart Hearing Aid." Technofocus. pp.38-41, 2016.

[17] A. O. Owojori, I. A. Adebanjo, and S. A. Oyetunji, "Design analysis of a mobile-based gait analyzer." European Journal of Electrical and Computer Engineering (EJECE), 3(3), pp.1 – 8, 2019.

[18] A. O. Owojori, T. O. Otunniyi, and E. O. Ogunti, "Digital Front-End for Software Defined Radio Wideband Channelizer." Communications on Applied Electronics Journal, 1(6), pp.25-35, 2015.

[19] B. Lin, P. Yang, C. Liu, Y. Huang, C. Liu, and B. Lin, "Design of Novel field programmable gate array-based hearing aid." IEEE Access, 7, 6380-63817, 2019. https://doi.org/10.1109/ACCESS.2019.2916723.

[20] A. O. Owojori, H. O. Alade, and A. O. Olotuah, "Analysis of an Automatic Sliding Window." Journal of Electrical Engineering, Electronics, Control and Computer Science (JEEECCS), 7(4), issue 26, pp. 9 – 16, 2021b.

[21] A. O. Owojori, A. M. Akinbolade and K. F.Akingbade, "Design Analysis of an Automatic Phase Selector." Journal of Engineering Studies and Research, 27(3), pp.51 – 63, 2021c.

[22] A. O. Owojori, J. O. O. Mebawondu, and J. O. Mebawondu, "Design of an obstacle and location-based detector with microcontroller system." European Journal of Electrical Engineering and Computer Sciences (EJECE), 5(2), pp.55 – 62, 2021a.

[23] A. O. Owojori and O. Adepoju, "Design of an Arduino-Based Pen Plotter System." Journal of Engineering and Engineering Technology. 18(1), pp.1-8, 2024. FUTAJEET, ISSN: 1598-0271.

[24] P. Narkhede, S. Poddar, R. Walambe, G. Ghinea, and K. Kotecha, "Cascaded Complementary Filter Architecture for Sensor Fusion in Attitude Estimation." Sensors. pp.1-18, 2021. https:// doi.org/10.3390/s21061937.

[25] M. A. Yusuf, U. S. Zainab, M. I. Ilyasu, I. B. Shehu, I. H. Jibrin, S. Abdullahi and A. Adedeji, "Design and Construction of Hearing Aid Device." IOSR Journal of Environmental Science, Toxicology and Food Technology (IOSR-JESTFT), 5(3), pp. 55-61, 2013, e-ISSN: 2319-2402,p- ISSN: 2319-2399